Histol Histopath (1988) 3: 301-314

Histology and Histopathology

Cytotoxic effects of 3-methylindole on alveolar epithelial cells and macrophages: with special reference to microtubular and filamentous assemblies in alveolar type I cells of bovine lung

Onkar S. Atwal, Kanwal J. Minhas and Michael S. Perry
Department of Biomedical Sciences, Ontario Veterinary College, University of Guelph, Guelph, Ontario, Canada

Summary. The alveolar type I cell is a major permeability barrier between the pulmonary interstitium and alveolar spaces and its thin cytoplasmic processes are greatly susceptible to injury. These cells are often observed to undergo progressive vesiculation, vacuolization and desquamation during 3-methylindole (3MI)-induced acute pulmonary edema after oral administration in goats and cattle. The present study describes proliferation of SER and the presence of polymerized tubulin in the form of microtubules arranged in large bundles shown at ultrastructural level as well as with immunofluorescence staining for tubulin in alveolar type I cells 72 hours after 3MI treatment. Such changes were not seen in pulmonary endothelial cells, alveolar type II cells, alveolar macrophages and neutrophils. The possible role of microtubules in alveolar type I cell as a mechanistic support to resist disruption against the forces of interstitial and alveolar edema is compared with alveolar type II cells, alveolar macrophages and neutrophils. The latter cells undergo dynamic movements in response to inflammatory stimuli and therefore did not show microtubules in their cytoplasm.

Key words: Alveolar epithelium, Cytotoxicity, Microtubules, Repair

Introduction

3-Methylindole (3MI) is a ruminal fermentation product of tryptophan. The toxic effect of 3MI on the ruminant lung is characteristic of a xenobiotic compound which undergoes conversion into highly reactive metabolites (Yokoyama et al., 1975; Carlson and Dickinson, 1978). Evidence suggests that 3MI is actively metabolized in the lung by mixed-function oxidase (MFO) system (Hammond and Carlson, 1976; Bray and Carlson, 1979; Bray and Atwal, 1980) and results in the production of reactive intermediates which covalently bind to tissue macromolecules. It is further suggested that metabolic activation of 3MI to highly electrophilic intermediates may be fundamental to the pathogenesis of 3MI-induced pulmonary damage. The possible cellular sites of MFO-mediated metabolism of 3MI are non-ciliated bronchiolar (Clara) cells and alveolar type I cells (Bradley, 1977; Huang et al., 1977; Bradley and Carlson, 1980). Smooth endoplasmic reticulum (SER) appears to proliferate before these cells undergo severe damage in the goat lung 24 to 48 hours after oral and/or intravenous administration of 3MI. Comparable results have been shown in cattle where SER proliferation in alveolar type I cells was demonstrated 24 to 48 hours after oral administration of 3MI (McLaren, 1983).

In pathophysiological terms, pulmonary edema is a single most important factor in determining the severity of 3MI-pneumotoxicity. The edema is preceded by degeneration, necrosis and desquamation of alveolar type I cells and non-ciliated bronchiolar epithelial cells. Between 48 and 96 hours post-dosing, edema is largely resolved, although hyaline membranes and fibrinous deposits may remain in the alveoli. In concurrence with these changes alveolar type II cells proliferate rapidly to replace exfoliated type I cells (Breeze and Carlson, 1982). According to Breeze and Carlson (1982), proliferation of bronchiolar epithelial cells also takes place during this period, but is overshadowed by alveolar response.

In our recent histopathological and ultrastructural studies, a single oral dose of 3MI produced vascular lesions composed of acute vasculitis, loss and replication of endothelial cells, disruption and muscularization of the intima, thickening of the media, and storage of glycogen in smooth muscle cells of intraacinar arteries and veins 72 hours posttreatment (Atwal and Persofsky, 1984a; Atwal and Persofsky, 1984b). Similar changes have previously been described in various types of

Offprint requests to: Dr. O.S. Atwal, Department of Biomedical Sciences, University of Guelph, Guelph, Ontario, N1G 1W2, Canada

hypertensive vascular disease (Herget and Palecek, 1978; Migally and Tucker, 1982). Subsequently, *in vitro* and *in vivo* experiments were carried out to evaluate the effects of 3MI on the bovine pulmonary vasculature. Pharmacologic use of nor-epinephrine on intrapulmonary artery strips in *in vitro* experiments indicated a severe inhibition of alpha adrenoceptor function (Perry et al., 1985). Parallel *in vivo* physiological data (pulmonary arterial pressure, pulmonary wedge pressure, systemic arterial pressure, cardiac out put) suggest that 3MI-induces a progressive pulmonary hypertension up to 72 hours following single oral dose of 3MI (Perry, 1986).

Clinically, salient features of pulmonary distress appears 8 to 12 hours after 3MI administration. After 20 hours, clinical signs include dyspnea and a marked expiratory grunt. A partial remission of these clinical signs is seen between 30 and 45 hours after 3MI administration. By 72 hours, animals undergo decompensation and clinical signs of severe dyspnea, depression and loud expiratory grunts are once again more pronounced.

Kinetic studies of 3MI metabolism have shown that it is rapidly absorbed from the rumen into the bloodstream. Ninety percent of an oral dose of 3MI is excreted within 72 hours as at least 10 urinary metabolites (Breeze and Carlson, 1982), yet animals show severe symptoms of pulmonary distress parallel with acute pulmonary hypertension 72 hours posttreatment. It appears therefore, that pulmonary parenchyma, especially the alveolar-capillary membrane is still under considerable stress at this time.

In consideration of this hypothesis, the present study was designed to investigate ultrastructural responses in alveolar type I cells, and pulmonary endothelium during actue alveolitis and pulmonary edema, 72 hours after oral administration of 3MI. The evidence is presented that in the present experimental system, alveolar-capillary membrane showed cytotoxic effects in the form of microtubular aggregation in the alveolar type I cells, severe vasculitis with intravascular and extravascular fibrinous deposits, neutrophil infiltration and hyperactive alveolar macrophages. The pulmonary endothelium, alveolar macrophages, as well as alveolar type II cells did not show any signs of microtubular assembly, especially in alveolar type I cells, has not been demonstrated nor has it ever been discussed relative to its importance during the reparative process of alveolar lining in disease condition of the mammalian pulmonary system (Bedrossian et al., 1973; Faulkner et al., 1973; Hirai et al., 1977; Huang et al., 1977).

Materials and methods

A mixed group of seventeen cattle primarily of beef breeds ranging from 1/2 years to 2 years of age and weighing approximately 225 kg were used in this study. Six cattle were purchased locally from the breeding farms and eleven cattle were supplied by Elora Research Station Farm of the University of Guelph. During the period of acclimatization, one animal developed acute pneumonia and was treated with several doses of antibiotics. After complete recovery the animal was used as a control. 3MI was purchased from Sigma Chemical Company. Eleven animals were given an oral dose of 0.1 to 0.2 gm/3MI/kgm of body weight in large gelatin capsules which were administered as a single dose. Six animals were used as controls. All animals were euthanized by an overdose of pentobarbital sodium, 72 hours after the oral treatment. The severity of pulmonary disease was evaluated clinically and by gross, light microscopic and electron microscopic examination. Four blocks of lung tissue were immediately removed from each lobe of control and treated animals. From each block, ten smaller pieces of tissue were prepared for electron microscopy and the rest were fixed in 10% buffered formalin for light microscopic examination. Paraffin sections were prepared by standard techniques and were stained with PAS hematoxylin method. For electron microscopy, lung samples were diced into 1 mm cubes in 2% glutaraldehyde in 0.1 M sodium phosphate buffer, pH 7.4. The tissue was washed in three changes of cold phosphate buffer, pH 7.4, post fixed in buffered 1% osmium tetroxide for one-half hour, dehydrated in ethanol and propylene oxide, and embedded in Epon 812. Thick sections were stained with toluidine blue, thin sections were stained with lead citrate and satured aqueous uranyl acetate and examined with a JEOL-200 electron microscope.

Immunofluorescence Staining

The tubulin antibodies were a kind gift from Dr. Eric Ball, Department of Biochemistry, University of Western Ontario, London, Ontario, Canada, and were used at a dilution of 1:40. Fluorescein conjugated goat-anti-rabbit IgG was obtained from Cappel Laboratories Inc. (Cochranville, PA). Small pieces of lung tissue were quickly frozen in isopentane at −100C and embedded in Tec II medium. Sections (5 μm) were dipped into a 3.5% paraformaldehyde solution in PBS for 10-20 minutes and then kept in a humidified chamber to prevent drying. Sections were quenched with 0.1M glycine in PBS for 4 to 5 minutes and then covered with 20 ml of anti-tubulin serum previously diluted 1:40 PBS. The treated sections were incubated in a humidified chamber at 37C for 20 minutes. Sections were rinsed 4 times for 5 minutes each with PBS and counterstained with fluorescein conjugated goat-anti-rabbit IgG at a dilution of 1:16 and incubated at 37C for 30 minutes. After rinsing again 4 times for 5 minutes each with PBS, samples were mounted with permount containing paraphenamine diamine. Excess mountant was blotted away and sections were viewed in a Zeiss universal microscope using transmitted illumination. Photomicrographs were taken with Kodak Tri-X pan film.

Results

Clinical signs, histopathological changes and

ultrastructural pathology of 3MI-induced respiratory disease 72 hours after treatment have been described in our previous reports (Atwal and Persofsky, 1984a; Atwal and Persofsky, 1984b). However, in the present study the changes were mostly comprised of interstitial and intraalveolar edema with characteristic intravascular, interstitial and intraalveolar fibrinous deposits. Microembolization and sequestration of leukocytes, platelets and erythrocytic aggregation were the predominant features of vascular changes. Alveolar type I cells showed increased vesiculation and vacuolization in a progressive manner before undergoing disruption, leaving the basal lamina completely denuded at several places. Alveolar type II cells showed signs of hyperplasia.

The major emphasis of the present study is focused on the description of pulmonary endothelium, ultrastructural changes in the remaining intact alveolar

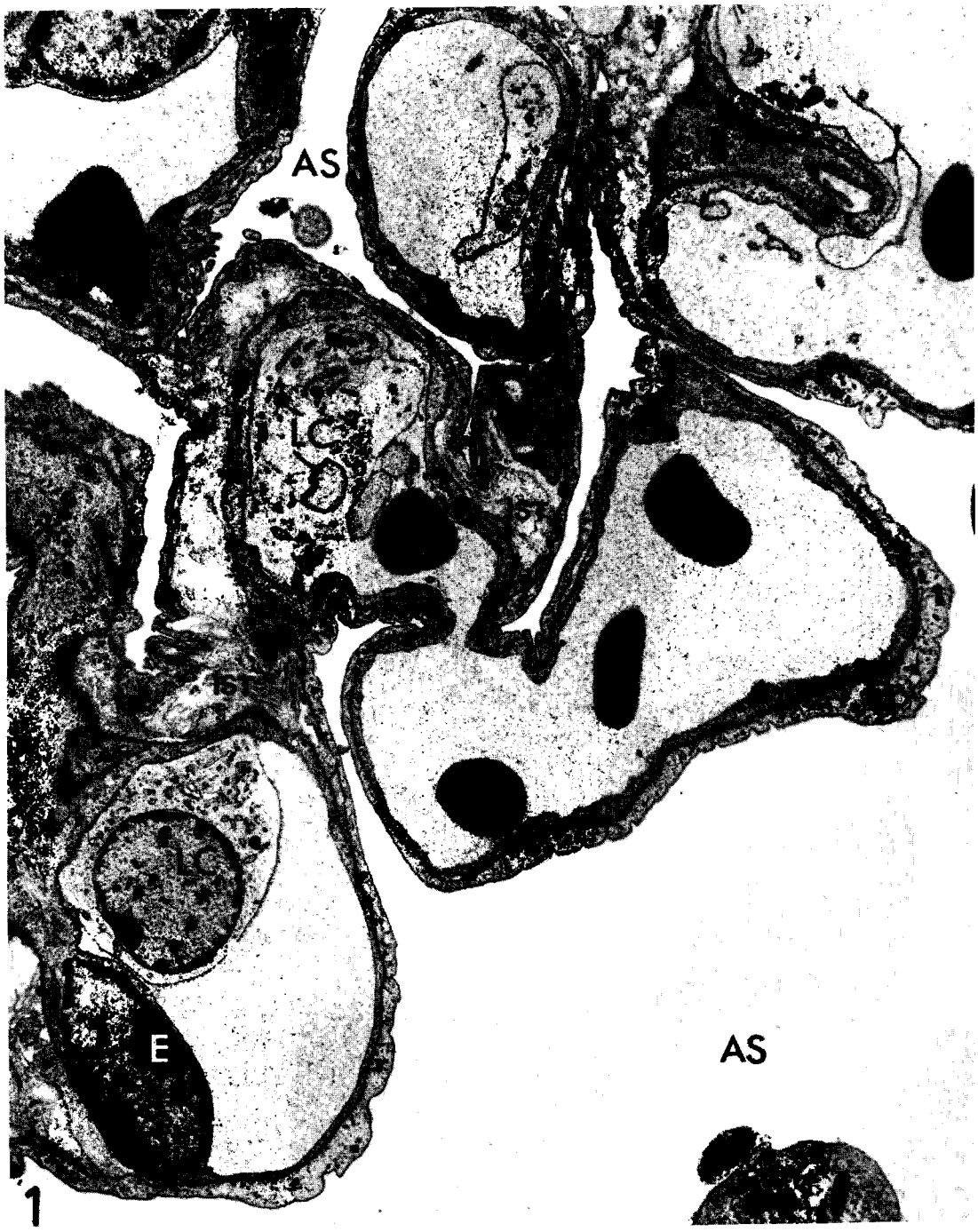

Fig. 1. Alveolar septums of a control lung show centrally placed capillaries, intravascular leukocytes (LC) and a few erythrocytes. Alveolar interstitium (IST), endothelium (E) and squamous alveolar type I cells (Ep) are also depicted. Note the abundance of cell organelles (asterisk) in the pulmonary endothelium.
As - alveolar spaces.
x 5,000

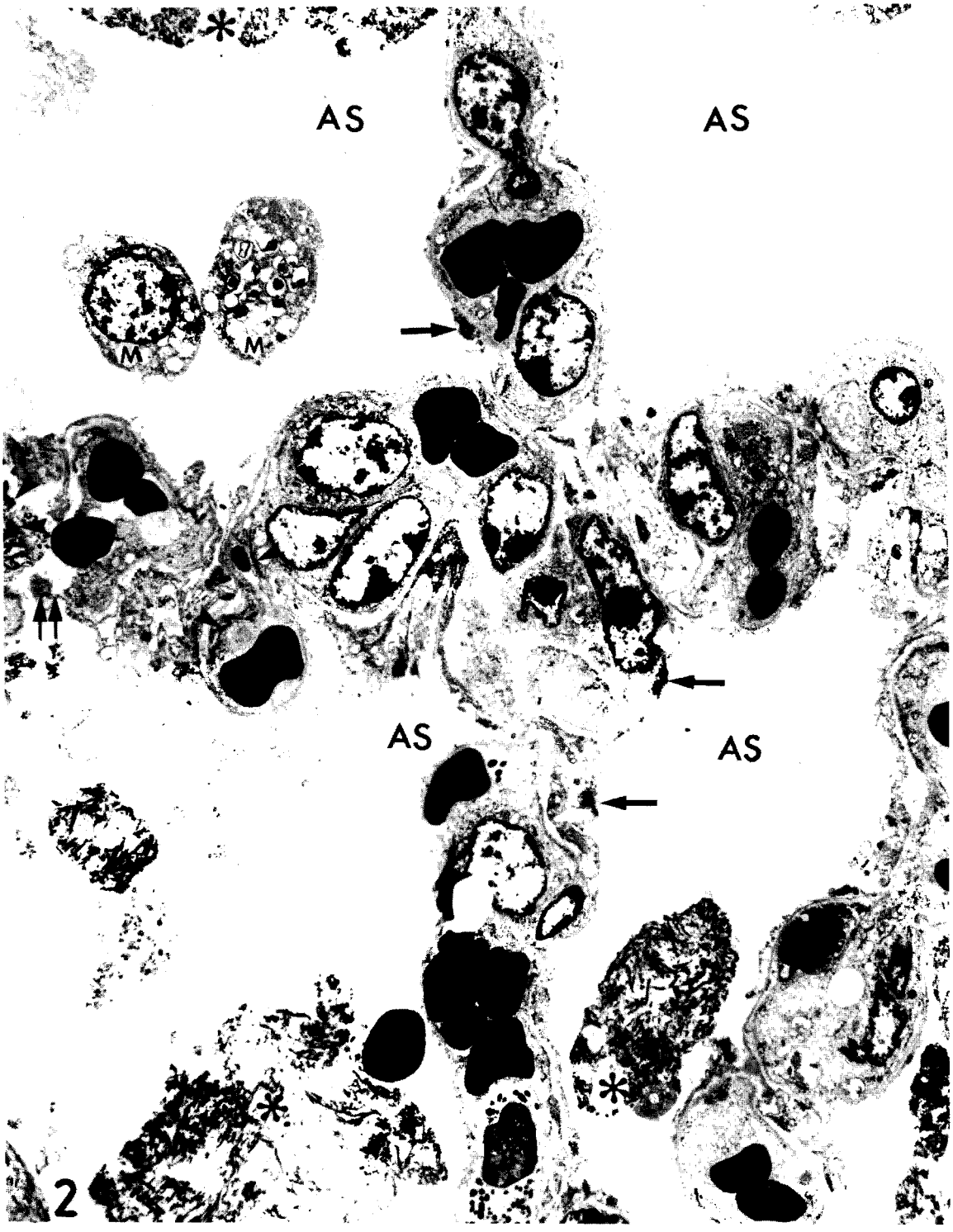

Fig. 2. Alveolar parenchyma of 3MI treated heifer shows fibrinous exudate (asterisks) in alveolar spaces (AS) as well as electron dense material of similar appearance inside the capillaries (arrowheads). Alveolar type I cells (arrows) are highly vacuolated and at various places are separated from the basal lamina. Alveolar capillaries are disrupted (double arrows) while vascular lumens are packed with emboli. x 2,500

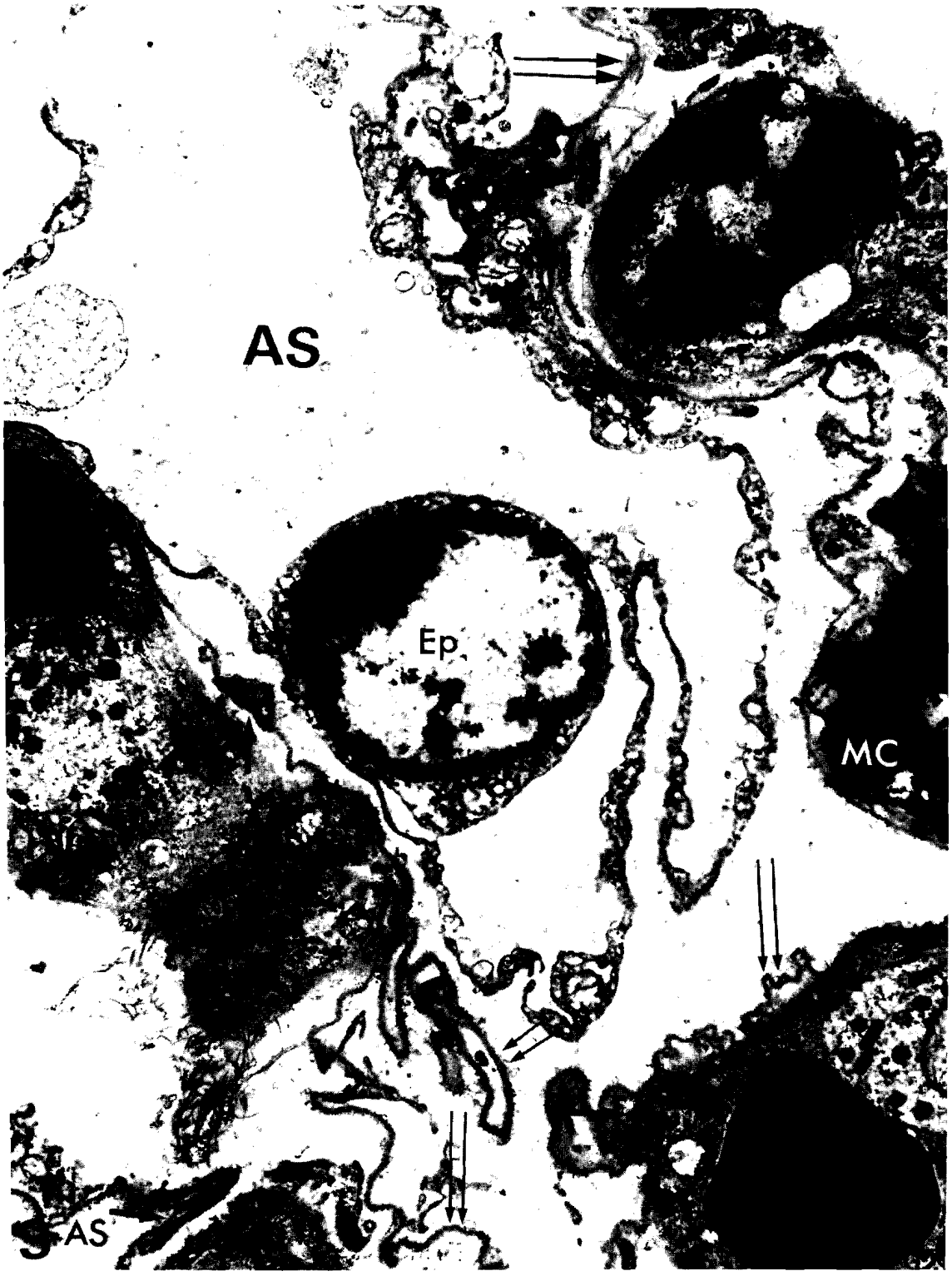

Fig. 3. A partially desquamated alveolar type I (Ep) cell has left behind a highly folded basal lamina (double arrows). The extent of undulation of basal lamina seems to be related to its distance from the lifted portion of the cell. Note the presence of electron dense precipitate in the alveolar interstitium especially in the juxtacapillary positions (thick arrows). AS - alveolar spaces; MC - mast cell. 3MI-treated animal. x 7,500

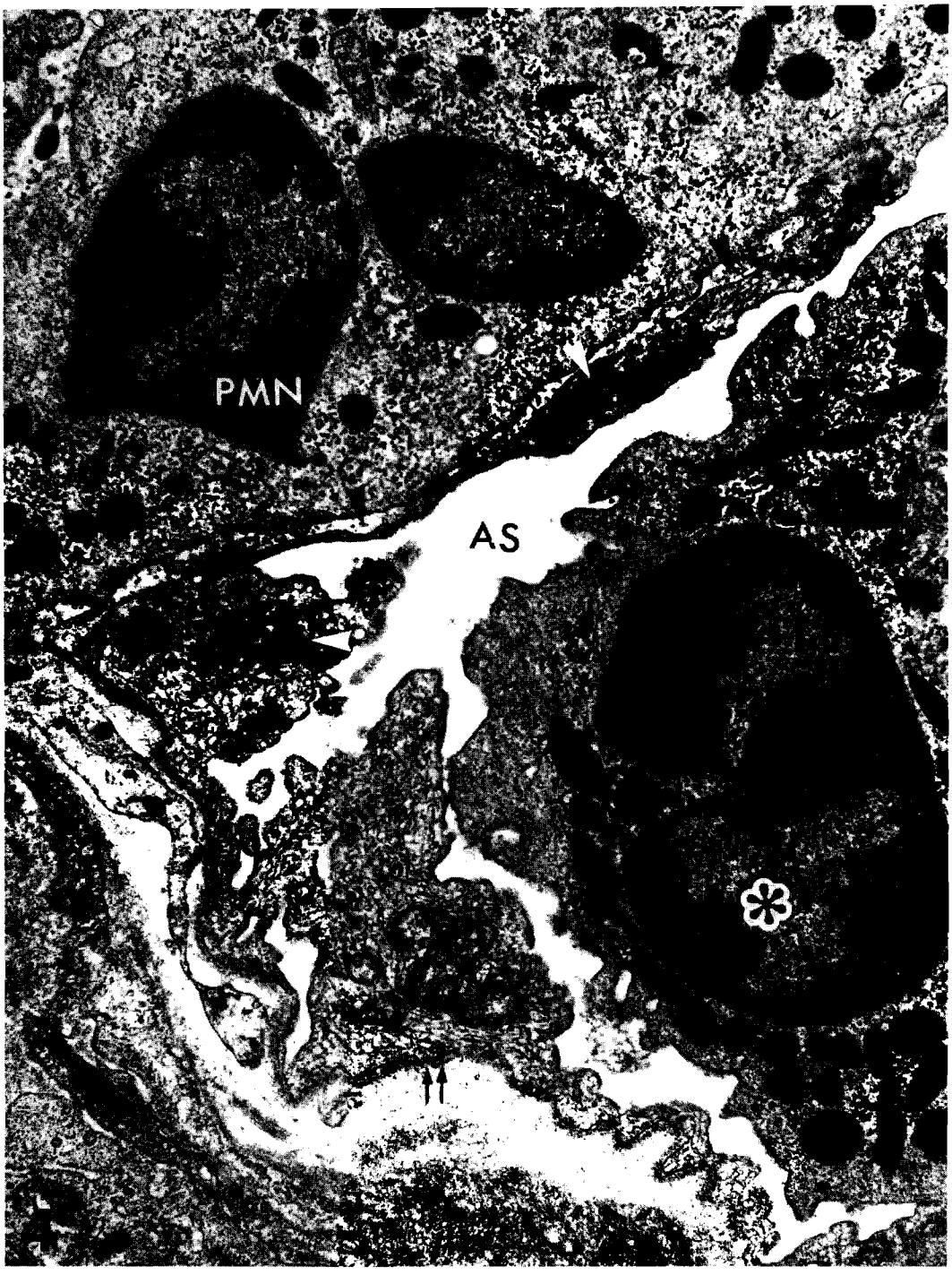

Fig. 4. A portion of an alveolar type I cell is resting on its basal lamina (double arrows) which has completely disappeared from the interface between a neutrophil (PMN) and its basal plasma membrane (black arrowheads). Note extensive distribution of SER, microtubules (white arrowheads) and mitochondria (M) in the epithelial cell. A neutrophil (asterisk) is lying in the alveolar space and contains a centriole (Ct). x 20,000

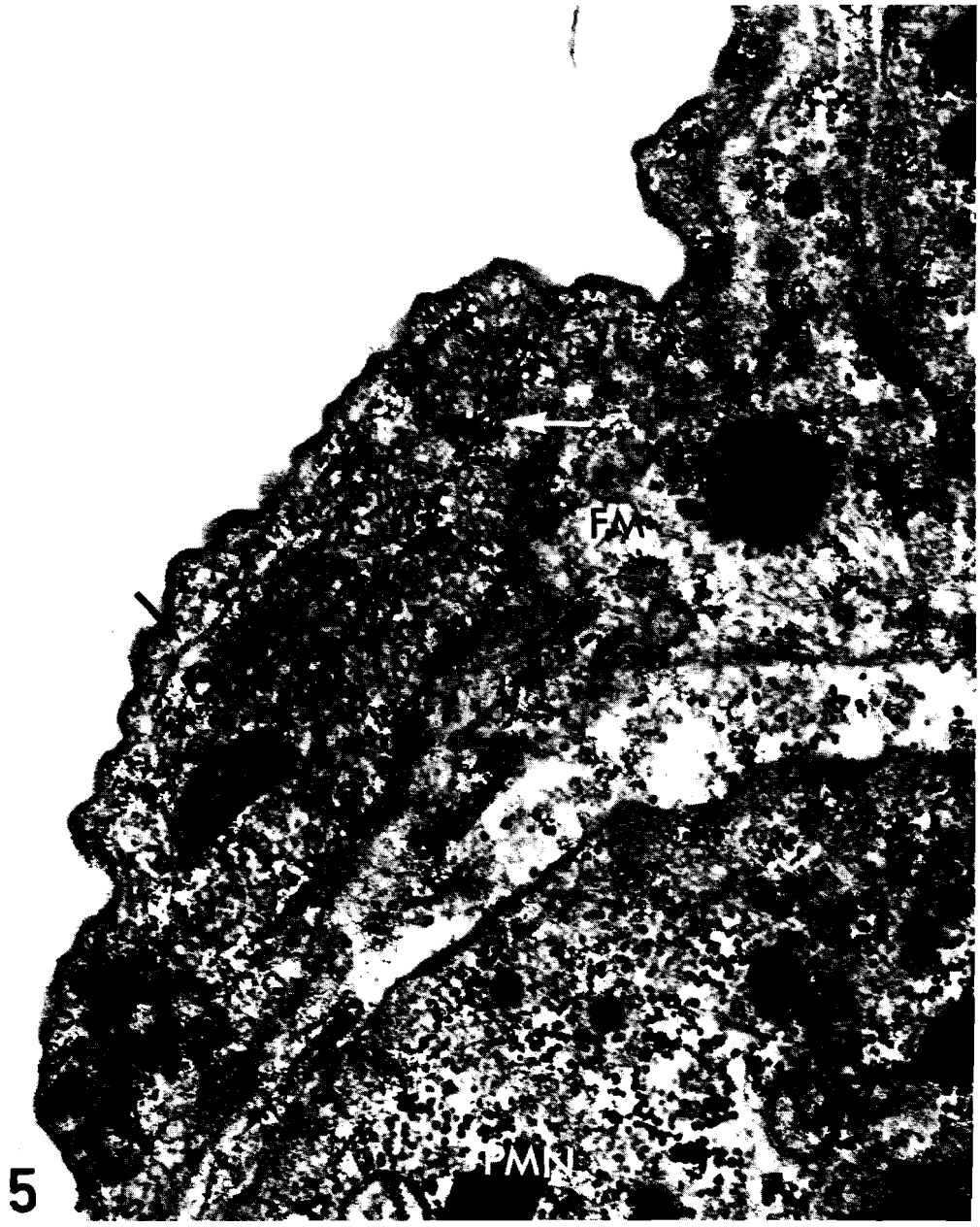

Fig. 5. A portion of an alveolar type I cell contains a mixture of large number of haphazardly arranged microtubules (black arrows) and intermediate filaments (10 nm) (white arrow). At left bottom of the picture some microtubules are obscured with proteinaceous material. Glycogen beta particles in the cytoplasm of a neutrophil (PMN) and a fibromuscular (FM) cell are also depicted. These cells also contain a few microtubules in their periphery. x 25,000

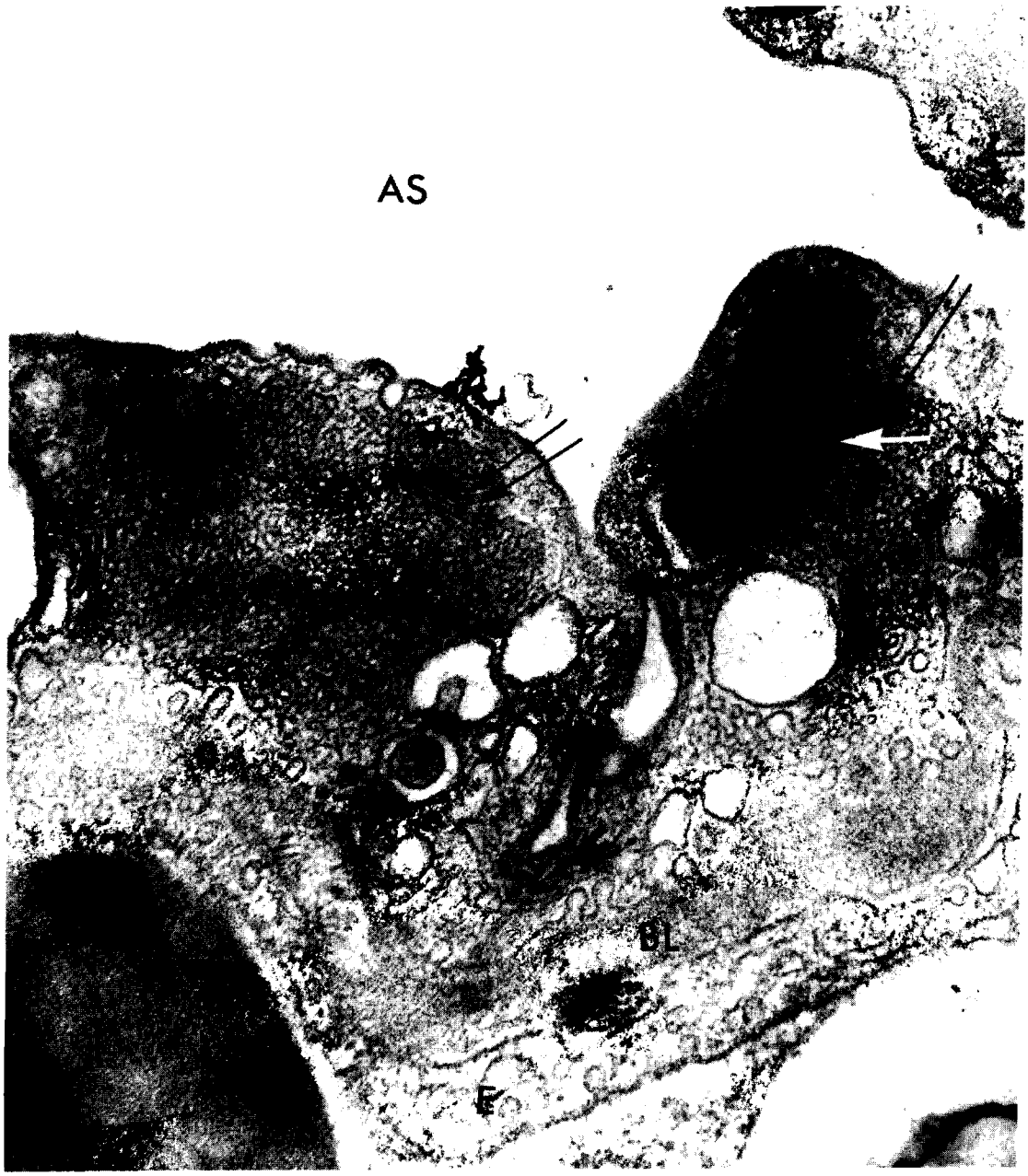

Fig. 6. A portion of an alveolar type I cell contains two large aggregates of microtubules. A few microtubules (thin arrows) are shown in a longitudinal section. A large number of MTBs appear to be obscured with proteins (white arrow). A few vesicles of SER and transport vesicles are seen intermixed with microtubules. BL - composite basal lamina of alveolar-capillary membrane; E - endothelium; AS - alveolar space. 3MI-treated animal. x 50,000

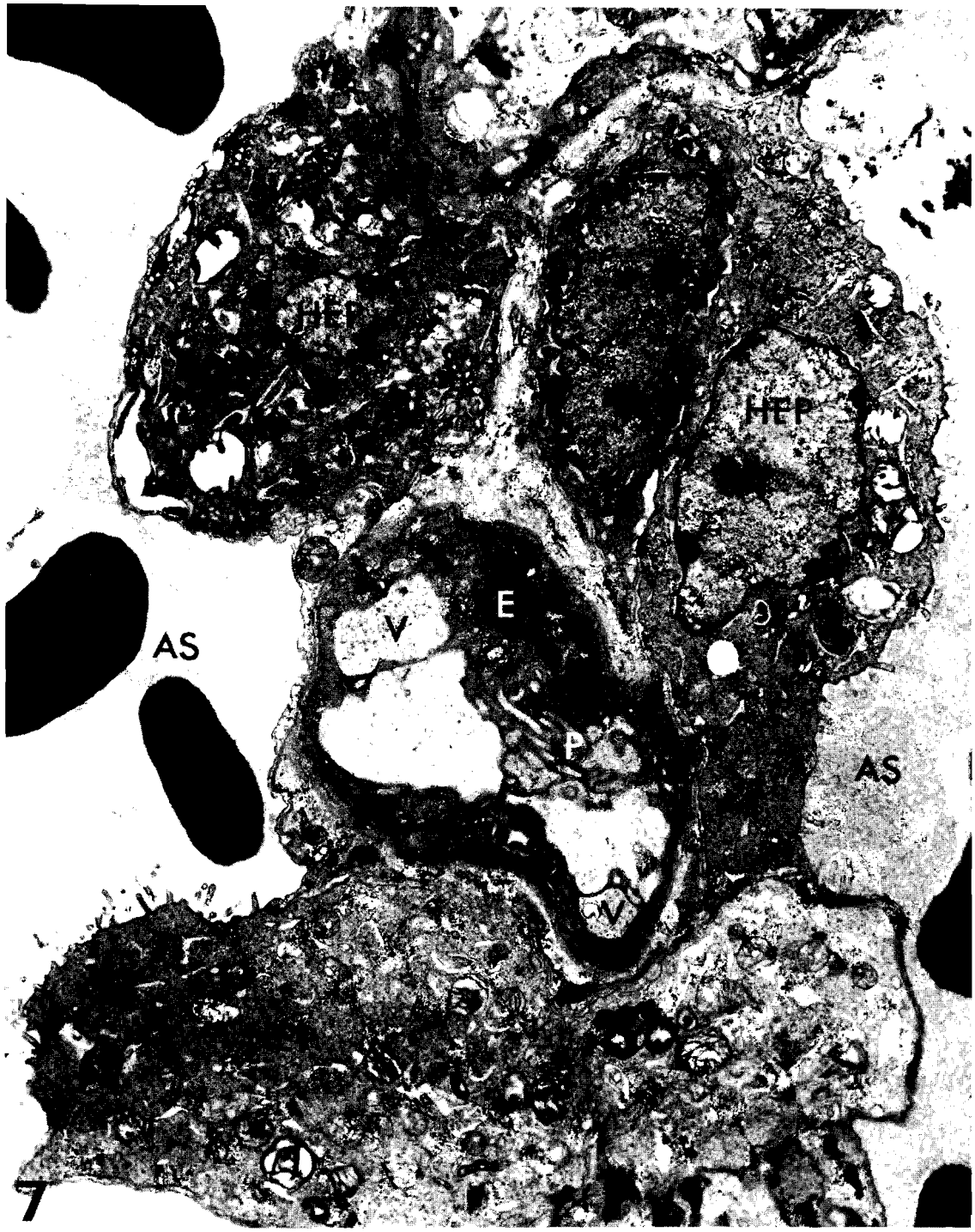

Fig. 7. Three hyperplastic alveolar type II cells (HEP) contain usual lamellar bodies, large amount of cytoplasm, mitochondria, free ribosomes, and tubular form of RER. Endothelium (E) of an alveolar capillary contains several papillary (P) and vesicular (V) processes arising from its luminal surface. Alveolar spaces (AS) contain a few erythrocytes. 3MI-treated animal. x 12,500

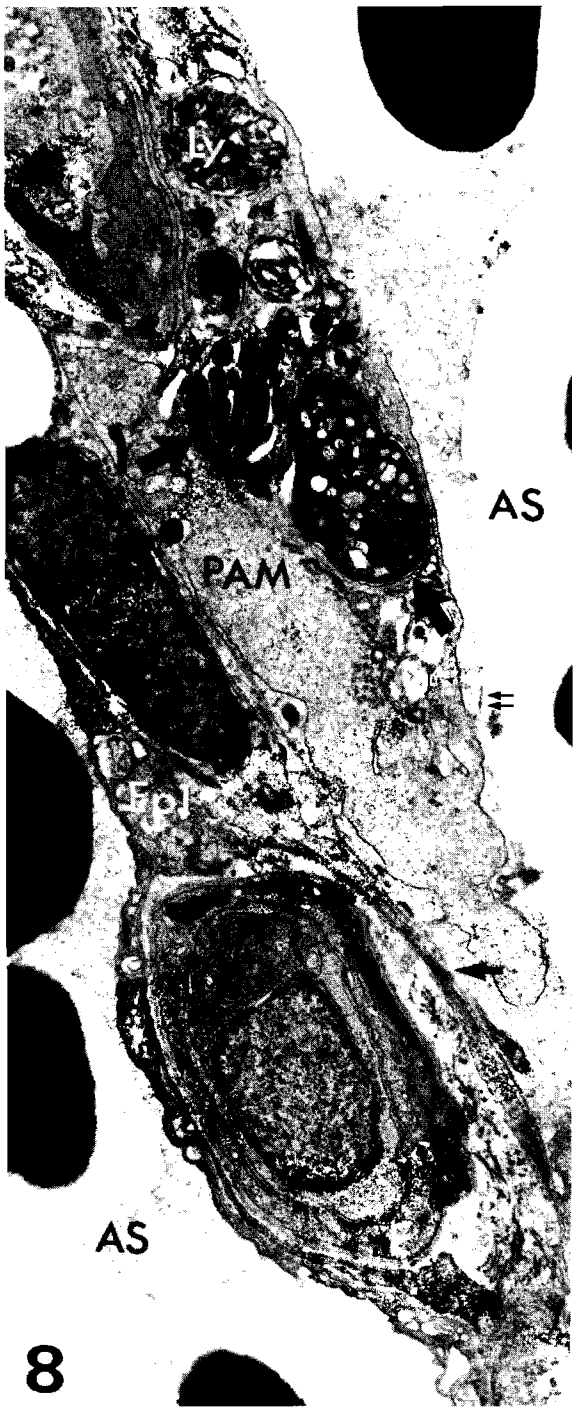

Fig. 8. An alveolar macrophage (PAM) lies in the hypophase layer of the surfactant (double thin arrows) and is seen invading the denuded basal lamina. It has also engulfed portions of disintegrated alveolar epithelium (thick arrows). Small pieces of epithelial cell-debris (arrow heads) are still seen against the basal lamina (arrow). E - endothelium of a capillary; Ep 1 - alveolar type I cell. AS - alveolar spaces; LY - a tertiary lysosome. 3MI-treated animal. x 10,000

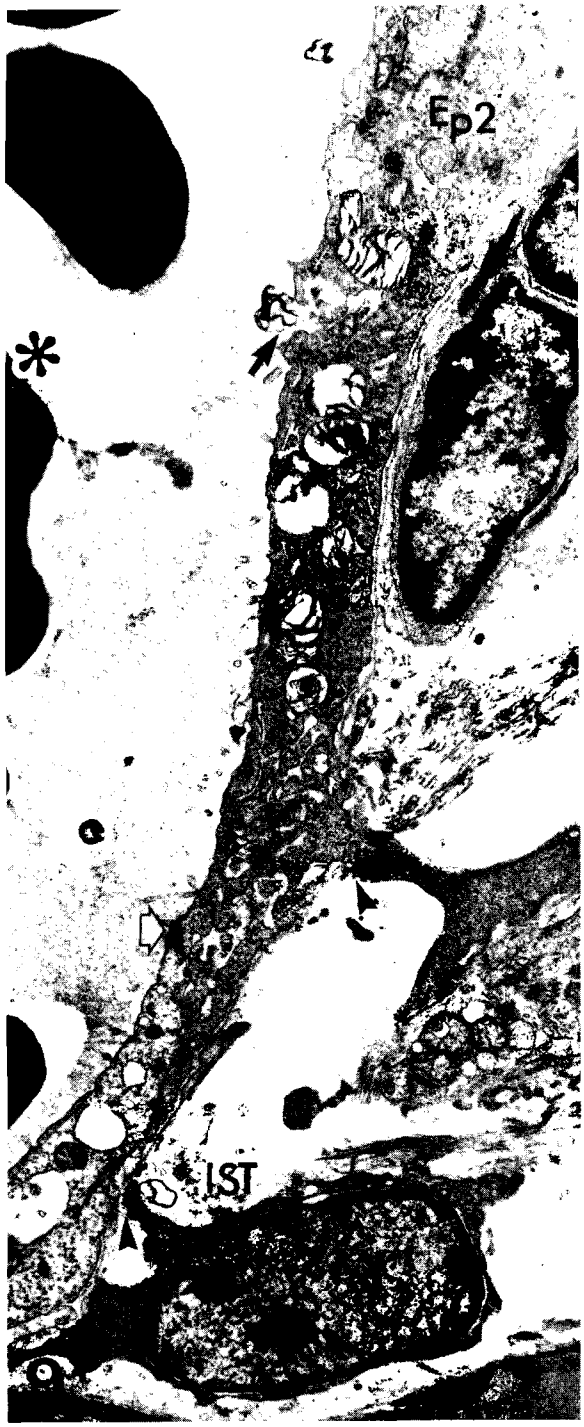

Fig. 9. The alveolar type II cell (Ep 2) is seen stretched along the basal lamina. This static view may represent the intermediate stage of differentiation into a squamous cell. A lamellar body is seen undergoing exocytosis (arrow) while several other lamellar bodies still occupy a large portion of cell cytoplasm. Alveolar (asterisk) and interstitial edema (IST), interepithelial cleft (open arrow) and foot processes of interstitial cells making contacts with basal lamina (arrowheads) are also depicted. 3MI-treated. x 7,500

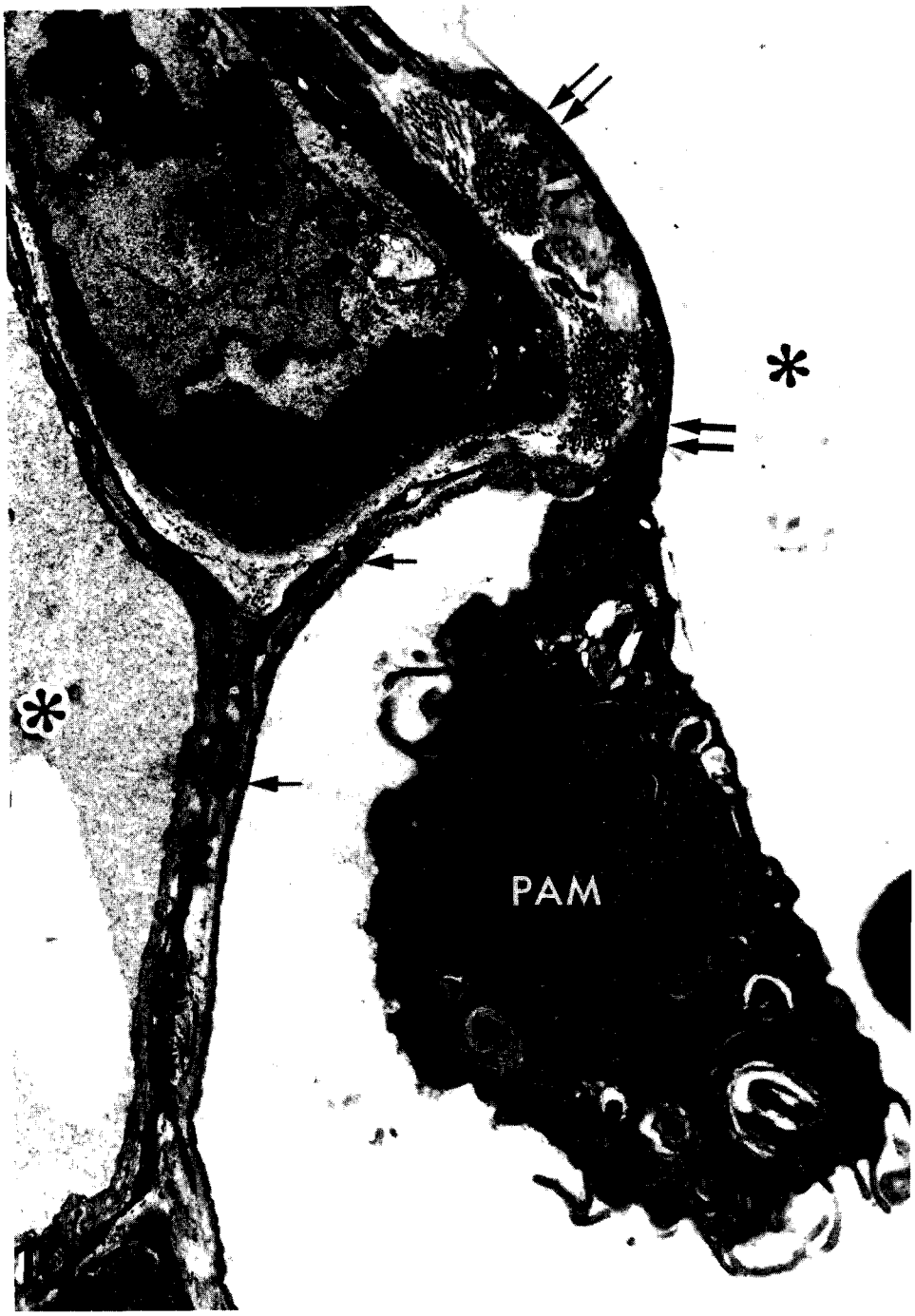

Fig. 10. A long thin lamellipod (thick double arrows) arises from the leading edge of an alveolar macrophage (PAM). It has formed an attachment (arrowheads) with an underlying attenuated alveolar type I cell (small arrows). Alveolar capillary (CAP) is packed with white blood cells with lipid inclusions. x 15,000

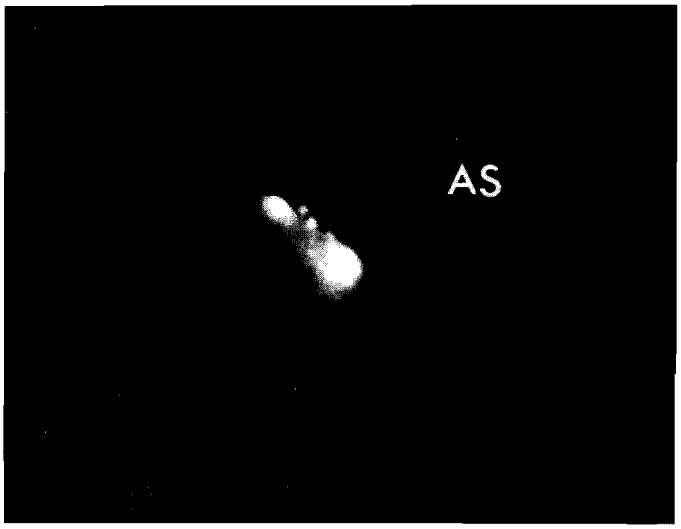

Fig. 11. Immunofluorescence staining for tubulin shows intense reaction in alveolar type I cell of 3MI-treated lung tissue. AS - alveolar space. x 250

type I cells, alveolar macrophages and neutrophils. In more specific terms, it deals with aggregation of microtubules and intermediate filaments, desquamation of alveolar type I cells and invasion of the alveolar wall by neutrophils and alveolar macrophages.

The changes occuring in the cytoskeleton of alveolar type I cells were closely compared with alveolar type II cells, alveolar macrophages and intravascular, interstitial, and intraalveolar neutrophils.

Pulmonary Capillaries and Endothelium

Alveolar septums of lungs of control animals contained centrally placed capillaries which were lined with nonfenestrated continuous type of endothelium. Broad cytoplasmic extensions contained unusual plasmalemmal vesicles intermixed with other organelles like endoplasmic reticulum, mitochondria and free ribosomes. Golgi complex was restricted to perinuclear cytoplasm, whereas large number of micro-tubules emanated from this area and spread into the extended portions of the endothelial cells. The preponderance of microtubules in the cytoplasm of endothelial cells was most conspicuous in sections suggestive of capillaries twisted around the septal connective tissue posts. In these situations, broad cytoplasmic extensions quite distant from the perinuclear zone, contained large number of plasmalemmal vesicles and linearly arranged microtubules (Fig. 1). The lumens were partially empty and contained occasional erythrocytes and leukocytes. Intravascular monocytes formed uropods and filipods and carried on their surface an electron-dense protein coat. No such features were associated with lympocytes and neutrophils.

Interstitium and Alveolary Type I Cells

Signs of severe vasculitis, interstitial edema, alveolitis and desquamation of alveolary type I cells were most conspicuous where large deposits of fibrin were present especially in the interstitium in juxtaposition to the epithelial basal lamina (Fig. 2). However, exfoliation of alveolar type I cells was not necessarily restricted to areas where vascular changes and interstitial disruption were of high magnitude. Exfoliation was also seen at such location where vascular damage was minimal and a least disruption of interstitial elements and epithelial cells occurred. At sites where alveolar type I cells were lifted-up, the basal lamina was severely folded. The intensity of undulation was more obvious where the epithelium had moved away from its scaffold (Fig. 3). At various points the basal plasma membrane of these cells was still seen glued to the underlined basal lamina (Fig. 3). A large number of neutrophils infilterated the interstitium with a concurrent loss of elastic fibers and basal lamina in their vicinity (Figs. 4-6). Glycogen particles of the beta type were seen scattered throughout the cytoplasm of neutrophils which had also infilterated the alveolar spaces. Alveolar neutrophils contained large accumulation of glycogen particles as well as cell organelles especially the Golgi complex, centrioles and associated microtubules (Fig. 4).

The most important features of alveolar type I cells were prominet SER, mitochondria and microtubular-arrays distributed in the form of large aggregates at different regions of the extended portions of the cytoplasm, especially in the areas where vascular lesions were less severe and epithelium had resisted desquamation from its basal lamina (Figs. 4-6). Concurrently, neutrophils and fibromuscular cells of the interstitium containing microtubules and filaments in their cortical areas were lying in close approximation to the epithelial basal lamina (Fig. 5). Several hundred or more microtubules were packed together, in bundles in the alveolar type I cells. The microtubular-aggregates occupied a large portion of the cell cytoplasm between the basal and apical plasma membranes (Fig. 6).

Alveolar Type II Cells and Alveolar Macrophages

Large surface area of the alveolar septums lost their epithelial lining and the basal lamina was left naked to be occupied by hyperplastic alveolar type II cells as well as invading alveolar macrophages (Figs. 7-10). Alveolar type II cells contained usual microvilli at the apical surface, lamellar bodies, a large amount of cytoplasm with RER, SER, ribosomes, mitochondria and microbodies. In direct contrast to alveolar type I cells, microtubules were not seen in the type II cell cytoplasm. Likewise, alveolar macrophages, during their invasion of alveolar septal surfaces were devoid of microtubular aggregates.

Alveolar macrophages were vigorously phagocytic for alveolar epithelium including alveolar type I and type II cells (Figs. 8, 10). They actively invaded the alveolar epithelium, especially alveolar type I cells, through their large lamellipods arising from their leading edges which formed attachment with the underlying epithelium (Fig. 10).

Immunofluorescence Microscopy

The specificity of the antibodies for tubulin was assessed by indirect immunofluorescence. Immunofluorescence microscopy of alveolar type I cells of 3MI-treated lung tissue showed intense staining for tubulin (Fig. 11). The identification of alveolar type I cells was based upon their littoral position which faced empty dark alveolar spaces filled sometimes with exudative fluid. The frequency of intensely stained cells in these positions, as well as the larger number of hyperplastic alveolar type II cells and free macrophages in the alveolar spaces observed at the histological and electron microscopic level were also used as positive clues in the identification of alveolar type I cells. Moreover, exfoliation of alveolar type I cells had further reduced their number, which explains the fact that positively stained cells were few and far between.

A weak staining was consistently observed in intersititial cells (most probably fibromuscular-

contractile cells) as well as in vascular and bronchiolar smooth muscle in both 3MI-treated and control samples. Although the level of staining in these cells was quite significant during visual examination, this level of fluorescence was invariably too low to be captured in film.

Frozen sections, which showed positive staining for tubulin in 3MI treated samples were subsequently stained with hematoxylin and eosin method immediately after photography. The cytology of the parenchymal tissue in these sections was not well preserved. Nevertheless, it was not impossible to differentiate lining squamous cells from alveolar type II cells and alveolar macrophages and to match these with positively stained cells in a similar position in immunofluorescent preparations.

Discussion

The present study describes at the ultrastructural level, large aggregates of microtubules in alveolar type I cells during acute alveolitis and pulmonary edema 72 hours after a single oral dose of 3MI in cattle. The morphological results correlated well with the immunofluorescent assay for microtubules. On the other hand, both methods of identification including assay for microtubules did not show similar results in alveolar type II cells, pulmonary endothelium, alveolar macrophages and the neutrophils. A wide variety of eukaryotic cells contain tubulin as a pool of unassembled dimeric units as polymerized tubulin in structured microtubules (Synder and McIntosh, 1976). The absence of demonstrable microtubules at an ultrastructural level and negative immunofluorescence staining for tubulin in cells other than alveolar type I cells is quite intriguing. Dimeric tubulin is thought to exist in a state of dynamic equilibrium with polymerized tubulin and this equilibrium could be shifted in either direction depending on the functional needs of the cell (Synder and McIntosh, 1976).

Recent investigations correlating the degree of polymerization of microtubule protein with surfactant secretion in alveolar type II cells have shown that an intact microtubule-microfilament system may be obligatory for enhanced surfactant secretion in culture and isolated perfused lung (Brown et al., 1986). Our *in vivo* study failed to show microtubules in alveolar type II cells in control as well as in 3MI-treated animals.

The behaviour of microtubules in endothelial cell culture has been investigated recently by means of immunofluorescence localization with antibodies to the subunit of microtubules. The bundles of microtubules emanate from the perinuclear region towards the cell periphery where microtubules tend to bend and run parallel to cell margin (Drenckhaham, 1983). According to Drenckhahn (1983), it is still not known whether microtubules in endothelial cells in situ have a similar distribution.

Examination of several samples of control animals at electron microscopic level during the present study revealed the presence of micro-tubules with orientation similar to that observed in endothelial cells *in vitro*. In this regard, the present ultrastructural evidence of microtubular array in the pulmonary endothelium with similar orientation to the *in vitro* model is of some interest.

Macrophages possess an extensive network of microtubules, demonstrable by electron microscopy and immunofluorescence with antitubulin antibody (Reaven and Axline, 1973; Frankel, 1976). The treatment of macrophages with colchicine or vinblastine, drugs which disrupt the microtubular assembly, causes a loss of polarized movement and subsequent replacement by vigorous ameboid motility (Pick and Abrahamer, 1973; Seger and Pick, 1984). In single cell organisms, movement of their tentacles is caused by rapid depolymerization of microtubules (Alberts et al., 1983), which during their inactive phase are packed together in large bundles. The present study shows that alveolar macrophages actively invaded the alveolar septal surface, but did not show polymerized tubulin in the form of microtubules. Recent studies have suggested that lymphokine and macrophage migration inhibitory factory (MIF), inhibit macrophage motility by promoting the assembly of microtubules (Pick et al., 1979). It seems, that microtubules stabilize eukaryotic cells and enable them to resist motility and disruption from their static position in order to perform their function (s) such as secretion, endocytosis, exocytosis and membrane transport, etc., by maintaining their dynamic polarity. Accordingly, the present ubiquity of microtubular assembly in intact alveolar type I cells perhaps ensure their resistance to disruptive forces of interstitial edema and pulmonary hypertension (Atwal and Persofsky, 1984; Perry, 1986). In the present context, the only cell which needs to maintain its integrity by preserving its topography in relation to its basal lamina is the alveolar type I cell. Physiologic evidence supports the concept that the alveolar epithelial- barrier offers substantial resistance to solute flux (Schneeberger, 1978; Pietra, 1984) by virtue of their junctions comprised of zonula occludens as impermeable seals, and low equivalent pore radii as compared to alveolar vessel endothelium (Gil, 1978). Other cells including alveolar type II cell, alveolar macrophages and neutrophils, all had to migrate and be mobile to divide, realign and repair damaged epithelial lining and to respond to chemotactic forces generated by inflammatory stimuli respectively.

In conclusion, the present morphologic appearance of microtubules in surviving alveolar type I cells is a unique feature, considering that these cells are known to be terminally differentiated cells and are not capable of replicating themselves; and lacking the resources to perform any secretory function (Schneeberger, 1978). Polymerized tubulin may be a contributing factor to their resistance to disrupting forces of interstitial and alveolar edema.

Acknowledgements. This study was supported by funds received from NSERC and the Ontario Ministry of Agriculture and Food.

Typing assistance of Ms. Julie Mason is gratefully acknowledged.

References

Alberts B., Cray D., Lewis J., Martin R., Keith R. and Watson J.D. (1983). The Cytoskeleton. In: Molecular Biology of the Cell. Garland Publishing Inc., New York, pp 549-609.

Atwal O.S. and Persofsky M.S. (1984a). Ultrastructural changes in intraacinar pulmonary veins. Relationship to 3-methylindole-induced acute pulmonary edema and pulmonary arterial changes in cattle. Am. J. Path. 114, 472-486.

Atwal O.S. and Persofsky M.S. (1984b). Ultrastructural pathology of intrapulmonary arteries in 3-methylindole-induced pneymotoxicity in cattle II. Glycogen accumulation in the smooth muscle cells and intimal changes. J. Path. 142, 141-149.

Bedrossian C.W., Luna M.A., MacKay B. and Lichtiger B. (1973). Ultrastructure of pulmonary bleomycin toxicity. Cancer 32, 44-51.

Bradley B.J. (1977). Electron and light microscopy of lungs and body distribution of carbon^{14}-3-methylindole in experimentally induced pulmonary edema and emphysema in goats. Doctoral thesis, Washington State University, Pullman, Washington.

Bradley B.J. and Carlson J.R. (1980). Ultrastructural pulmonary changes induced by intravenously administered 3-methylindole in goats. Am. J. Path. 99, 551-556.

Bray T.M. and Atwal O.S. (1980). Effect of energy restriction on mixed function oxidase activity and the development of acute pulmonary edema in goats. Fed. Proc. 39, 891.

Bray T.M. and Carlson J.R. (1979). Role of mixed function oxidase system in 3-methylindole-induced acute pulmonary edema in goats. Am. J. Vet. Res. 40, 1268-1272.

Breeze R.G. and Carlson J.R. (1982). Chemical induced lung injury in domestic animals. Adv. Vet. Sci. Comp. Med. 26, 201-231.

Brown L.A.S., Pasquale S.M. and Longmore W.J. (1986). Role of microtubules in surfactant secretion. J. Appl. Physiol. 58, 1866-1873.

Carlson J.R. and Dickinson E.O. (1978). Tryptophan-induced pulmonary edema and emphysema in ruminants. In: Effects of Poisonous Plants in Livestock. Keeler R.F., Vankampen K.R. and James I.F. (eds). Academic Press Inc. New York, pp. 261-272.

Drenckhahn D. (1983). Cell motility and cytoplasmic filaments in vascular endothelium. In: Progress in Applied Microvascular Structure and Function of Endothelial Cells. Vol. 1. MeBrmer K. and F. Hammersen F. (vol. eds.), Karger Basel, pp. 53-70.

Faulkner C.S. and Connolly K.S. (1973). The ultrastructure of 60_{Co} radiation pneumonitis in rats. Lab. Invest. 28, 545-553.

Frankel F.R. (1976). Organization and energy-dependent growth of microtubules in cells. Proc. Natl. Acad. Sci. U.S.A. 73, 2798-2802.

Gil J. (1978). Lung interstitium, vascular and alveolar membrane. In: Lung Water and Solute Exchange. Staub N. (ed.). Marcel Dekker INc. New York, pp. 49-73.

Hammond A.C. and Carlson J.R. (1976). 3-methylindole-metabolite excretion in goats. In: Proceedings Western Section. Am. Soc. Anim. Sci. 27, 332-334.

Herget J. and Palecek F. (1978). Experimental chronic pulmonary hypertension. Int. Rev. Exp. Pathol. 18, 347-406.

Hirai K.I., Witschi H. and Cote M.G. (1977). Electron microscopy of butylated hydroxytoluene-induced lung damage in mice. Exp. Mol. Path. 27, 295-308.

Huang T.W., Carlson J.R., Bray T.M. and Bradley B.J. (1977). 3-methylindole-induced pulmonary injury in goats. Am. J. Pathol. 87, 647-658.

Keiser H.D. (1980). The effect of lysosomal enzymes on extracellular substrate. In: The Cell Biology of Inflammation. Weissman G. (ed). Elsevier/North Holland Biochemical Press, Amsterdam, pp. 431-468.

Migally N., Tucker A. and Zambernord J. (1982). Glycogen localization in pulmonary vascular smooth muscle of chronically hypoxic rats. J. Submicroscop. Cytol. 14, 247-252.

McLaren J.M. (1983). A morphological study of 3-methylindole induced pneumotoxicity in cattle. M.Sc. thesis, University of Guelph, Guelph, Ontario.

Perry M.S., Atwal O.S. and Eyre P. (1985). Impairment of sympathetic pulmonary vasoconstriction by 3-methylindole in cattle. Am. J. Vet. Res. 46, 905-908.

Perry M.S. (1986). Correlative pathophysiological study of 3-methylindole-induced pneumotoxicosis in cattle. Ph.D. Thesis, University of Guelph, Guelph, Canada.

Pick E. and Abrahamer H. (1973). Blocking of macrophage migration inhibitory action by microtubular disruptive drugs. Int. Arch. Allergy Appl. Immunol. 44, 215-220.

Pick E., Honing S. and Griffel B. (1979). The mechanism of action of soluble lymphocyte mediators. VI. Effect of migration inhibitory factor on macrophage microtubules. Int. Arch. Allergy. Appl. Immunol. 58, 149-159.

Pietra G.G. (1984). Biology of disease: New insights into mechanisms of pulmonary edema. Lab. Invest. 51, 489-494.

Reaven E.P. and Axline S.G. (1973). Subplasmalemminal microfilaments and microtubules in resting and phagocytozing cultivated macrophages. J. Cell Biol. 59, 12-27.

Schneeberger E.E. (1978). The integrity of the air-blood barrier, The Respiratory Defence Mechanism, Vol. 5. Brain J.D., Proctor D.F. and Reid L.M. (eds.). Marcel Dikker Inc. New York, pp. 687-708.

Seger M. and Pick E. (1984). Macrophage microtubules: An optimized method for the assay of tubular concentration and state of polymerization in macrophages. Jour. Leukoc. Biol. 35, 303-316.

Synder J.A. and McIntosh J.R. (1976). Biochemistry and physiology of microtubules. Annu. Rev. Biochem. 45, 699-720.

Yokoyama M.T. and Carlson J.R. (1974). Dissimilation of tryptophan and related indolic compounds by ruminal microorganisms in vitro. Appl. Microbiol. 27, 540-548.

Yokoyama M.T., Carlson J.R. and Dickinson E.D. (1975). Ruminal and plasma concentrations of 3-methylindole associated with tryptophan-induced pulmonary edema and emphysema in cattle. Am. J. Vet. Res. 36, 1349-1352.

Accepted February 19, 1988